

Accepted Manuscript

Effect of steelmaking dust characteristics on suitable recycling process determining: Ferrochrome converter (CRC) and electric arc furnace (EAF) dusts

Mamdouh Omran, Timo Fabritius

PII: S0032-5910(16)30841-5
DOI: doi: [10.1016/j.powtec.2016.11.049](https://doi.org/10.1016/j.powtec.2016.11.049)
Reference: PTEC 12125

To appear in: *Powder Technology*

Received date: 12 October 2016
Revised date: 7 November 2016
Accepted date: 26 November 2016



Please cite this article as: Mamdouh Omran, Timo Fabritius, Effect of steelmaking dust characteristics on suitable recycling process determining: Ferrochrome converter (CRC) and electric arc furnace (EAF) dusts, *Powder Technology* (2016), doi: [10.1016/j.powtec.2016.11.049](https://doi.org/10.1016/j.powtec.2016.11.049)

This is a PDF file of an unedited manuscript that has been accepted for publication. As a service to our customers we are providing this early version of the manuscript. The manuscript will undergo copyediting, typesetting, and review of the resulting proof before it is published in its final form. Please note that during the production process errors may be discovered which could affect the content, and all legal disclaimers that apply to the journal pertain.

**Effect of steelmaking dust characteristics on suitable recycling process determining:
Ferrochrome converter (CRC) and electric arc furnace (EAF) dusts**

Mamdouh Omran^{a,b*}, Timo Fabritius^a

^a Process Metallurgy Research Group, Faculty of Technology, University of Oulu, Finland.

^b Mineral Processing and Agglomeration Lab, Central Metallurgical Research and Development Institute, Cairo, Egypt.

Abstract

Utilization of dusts generated from steelmaking industries will avoid disposal of wastes, enhance the use of secondary raw material fines and save costs. Understanding the properties of dust is necessary before determining the suitable recycling method. The present paper describes the chemical, morphological and mineralogical characterization of steelmaking dusts produced in steel plants in Finland. In this paper three different steelmaking dusts: ferrochrome converter (CRC) and electric arc furnace stainless steel (EAFSS) dusts from Outokumpu (Tornio, Finland), and electric arc furnace carbon steel (EAFCS) dust from Ovako (Imatra, Finland) were characterized.

The characterization study showed that, the dusts from carbon steelmaking (EAFCS) are rich in zinc, while the dusts from stainless steelmaking (CRC) and (EAFSS) are relatively low in zinc, but richer in chromium. The zinc contents in CRC, EAFSS and EAFCS dusts are 10.83, 19.84 and 35.76 wt.%, respectively, while the chromium contents are 20.88, 3.19 and 0.47 wt.%, respectively. In the dust from CRC, zinc is found as zinc oxide (zincite, ZnO), while in the dusts from EAFSS & EAFCS zinc is found mostly as zinc ferrite (franklinite, ZnFe₂O₄). Scanning electron microscopy (SEM) investigations indicated that CRC dust is dominated by non-spherical form and composed mainly of aggregates of irregular particles of chromite, in addition to zincite sphere. EAFSS dust particles are characterized by encapsulation phenomenon, franklinite particles enclosed inside calcium-iron-silicate glass sphere. Manganese (Mn) concentrations shows positive correlation with

Zn, which suggests the occurrence of Mn mainly with franklinite phase. EAFCS dust is dominated by spherical form, and zinc found as franklinite and zincite. In the large particles $> 3 \mu\text{m}$ of EAFCS dust, franklinite enclosed inside glass sphere, while in finer particles $< 1 \mu\text{m}$, both zincite and franklinite are existed as spheres.

The investigations indicate that steelmaking dusts from CRC, EAFSS, and EAFCS show significant difference in concentration and mode of occurrence of zinc in the dusts, which will influence on determine the suitable processing methods.

Keywords: Characterization; recycling; CRC; EAF; steelmaking dust.

Corresponding author:

Mamdouh Omran

Address: Process Metallurgy Research Group, Faculty of Technology, University of Oulu, Finland.

P.O. Box: 4300.

E-mail: mamdouh.omran@oulu.fi; mamdouh_nasr82@yahoo.com

1. Introduction

There are different types of steelmaking dusts generated from steel industries [1, 2], depending on process unit: stainless steel dust, carbon steel dust and ferrochrome dust. These dusts are by-product waste generated by the secondary steelmaking process in an electric arc furnace and considered as a hazardous waste in most industrialized countries [3, 4]. During the melting of scraps in the electric arc furnace (EAF), many components of the charge including iron, zinc, and lead, are volatilized and entered the vapour phase. The dust is formed through the conversion of vapour phases into dust by agglomeration and physico-chemical transformations, then the dust is collected in the off-gas cleaning system [5, 6]. Dust is fine-grained material, containing significant amounts of zinc and iron together with variable amounts of calcium, manganese, magnesium, silicon and chromium [7]. The composition of steelmaking dust depends on the type of the steel produce, scrap used and

operating conditions [7]. Zinc represents the major compound of the steelmaking dust, and its content varies between 7 and 40%, depending on scrap used, and the ratio of galvanized scrap utilized [8 – 10]. Compounds like zinc oxide (ZnO) and zinc ferrite (ZnFe_2O_4) are formed through interaction between vapour zinc and other gaseous compounds generated during the steelmaking process [5]. The direct recycling of dust back to steel production is hindered due to the presence of zinc, which cause operational difficulties in the steel making processes.

The present paper describes the chemical, physical, morphological and mineralogical characterization of steelmaking dusts produced in Finland steel plants and its implication on determine recycling methods. Characterization will include chemical analysis (composition and species), grain size distribution, microscopic observation, and definition of present mineral phases. Beside the chemical analysis, further methods are used to characterize the dust in detail; these are: Scanning electron microscopy (SEM) coupled with Energy-dispersive X-ray spectroscopy (EDS), Thermogravimetric - Differential scanning calorimetry (TG–DSC), Mass spectroscopy (MS), and Fourier transform infrared (FTIR) spectroscopy. Based on detailed characterization of dusts, a possible and most suitable method for recycling each kind of dust was proposed.

2. Materials and production process

Three representative steelmaking dust samples were used in this study. Ferrochrome converter (CRC) and electric arc furnace stainless steel (EAFSS) dusts were obtained from Outokumpu Tornio stainless steel plant, Finland. One dust sample came from electric arc furnace carbon steel (EAFCS) production from Ovako Imatra, Finland. The dusts were collected from bag house filter containers behind each furnace or converter. These dusts are a mixture of different production batches, so each dust is a representative sample of an average dust composition.

The flow sheet for the production processes in Outokumpu Stainless and Outokumpu Chrome Tornio is presented in Fig. (1). In Tornio plant, ferrochrome is produce in the same location from

chromite ore and concentrates as raw materials by using submerged arc furnaces (SAF). The molten ferrochrome can be transfer directly to the stainless steel plant [11, 12]. There are two production routes in Torino steel plant. In the Line 1 molten ferrochrome is fed as melt into ferrochrome converter (CRC), whereas in line 2 solid ferrochrome is melted with scrap in electric arc furnace (EAF) [11]. The charge weight of line 1 is 95 tonnes and line 2 is 150 tonnes. The Line 1 is using a chromium converter to treating liquid ferrochrome from ferrochrome melting shop. Whereas in line 2 electric arc furnace (EAF) is used to melt the scrap, this line is scrap-based stainless steelmaking. The ferrochrome converter (CRC) used as intermediate process between SAF and Argon oxygen decarburization (AOD) converter, because its product is a raw material for AOD [11, 13]. The raw materials for the CRC process are stainless steel scrap, and molten ferrochrome with high silicon and carbon content from the submerged arc furnace (SAF) of the ferrochrome plant [12]. The purpose of a ferrochrome converter (CRC) is to remove silicon and some carbon from molten ferrochrome by blowing oxygen into the melt before the production of stainless steel [11, 12]. The CRC process in Tornio generates about 4000 t a^{-1} of CRC dust. The liquid steel is charged into AOD converter to reach to the final quality of steel. The AOD is charged with molten ferrochrome from chromium converter (CRC) and molten steel from EAF. During the AOD process the oxygen and mixture of oxygen and nitrogen are injected to the melt to reduce the carbon, nitrogen and sulphur to specified limits. The AOD is followed by ladle treatments, continuous casting, slab grinding, hot and cold rolling as well as pickling and annealing [11].

The production processes in Ovako Imatra is shown in Fig. (2). Ovako Imatra is producing specials steel using steel scrap as raw material in electric arc furnace (EAF) with 75 tonnes capacity. Steel scrap is preheated and charged to EAF by two loaded buckets having typically 50 tonnes and 30 tonnes weights. Lime and crashed refractory bricks are used as slag formers and coke fines as reductant agent. EAF is equipped with lime and carbon injectors as well as oxygen- fuel burners. Typical tap-to-tap time is 65 minutes and total energy consumption about 38 MWh (32 MWh

electricity and 6 MWh chemical energy). Flue gas is cleaned during scrap melting process in two stages: large particle removed from dry flue gas and recycled back to process. Finer fractions are separated with bag filters. Typical generated dust volume is between 15 to 25 kg per ton of liquid steel [14]. The total amount of dust formation in Ovako Imatra about 2400 t a^{-1} and with higher production rate it could exceed 3000 t a^{-1} . The molten steel is going into secondary metallurgical process to remove sulphur and other impurities from the steel. The refined liquid steel goes to continuous bloom casting.

3. Characterization methods

The mineralogical composition of the samples were measured using Rigaku SmartLab 9kW at the centre of microscopy and nanotechnology of the University of Oulu. Before the X-ray diffractometer (XRD) analysis, the dust was pulverized in an agate grinding mortar. The XRD analyses were done using operating conditions of 40 kV accelerating voltage and a current of 40 mA with cobalt tube and a graphite monochromator. The measuring range from 4 to $90^\circ 2\theta$ using a step size of $0.02^\circ 2\theta$ and a step time of 1 s per step.

Bruker AXS S4 Pioneer X-ray fluorescence (XRF) spectrometer was used to determine the chemical composition of dust samples. The X-ray spectrometer equipped with Rh-tube with max power of 4kW. A selection of analyser crystals, detectors (flow counter and scintillation counter) and 66 geostandards were used for calibration of elements. About 13.16 g of ground sample was taken and mixed with 0.84 g of C-wax. WC/Co mortar HERZOG pulverizing mill was utilized to obtain homogeneous dispersion and uniform particle size of the resultant mixture (sorbent and C-wax). Pressed pellets for XRF analysis were prepared from the mixture (7–8 g) using boric acid as binder and applying a hydraulic pressure of 10 ton to compress the sample. The total carbon content of the dust is determined using a LECO Carbon Analyzer. The pH values of the dusts were measured after leaching 10 g of dusts with 25 mL of doubly deionized (DDI) water. The moisture

content of dust was calculated after drying a constant weight of dusts overnight at a temperature of 115 °C using stainless steel oven.

The morphological characteristic and microanalyses of the different zinc, iron, and chromium phases in the steel dust samples were investigated by a combined SEM-EDS using a Zeiss ULTRA plus field emission scanning electron microscope (FESEM), which was attached to an Energy-dispersive X-ray spectroscopy (EDS) unit for chemical analysis. Small amounts of the dust and liquid epoxy were placed into containers and the mixtures were dried until the material was solid. Then polished sections with a diameter of 25mm were prepared by cutting the samples vertically and polishing their surfaces. The granulometric analysis of the dust samples was determined using Beckman Coulter LS 13 320.

Infrared (FT-IR) Spectroscopy provides information about the structure and the nature of the functional groups present in the crystal lattice. FTIR was examined via Bruker Vertex V80 vacuum FT-IR spectrometer with Harrick Praying Mantis TM DRIFT equipment. The angle of incidence of the IR beam was 45° and 100 scans were collected at a resolution of 4 cm⁻¹. The spectral were collected within the range of 400–4000 cm⁻¹ wave number. Differential scanning calorimetry (DSC), Thermogravimetry (TG), and Mass spectra (MS) spectroscopy were used to determine the thermal behavior of steel dust samples. Thermogravimetry give information about the temperature-dependent mass loss of the sample, while mass spectroscopy detected the gases evolved during thermal reactions. The thermoanalyses was performed using a Netzsch STA409 PC Luxx under air atmosphere. Approximately 30.84 mg of sample was placed in a platinum crucible on a pan of the microbalance at a heating rate of 20 °C/min. The temperature range was 20–1400 °C.

4. Results and Discussion

4.1. Granulometric analysis

The granulometric distribution analyses and the median particle size for CRC, EAFSS and EAFCS dusts are shown in Figs. (3 – 5) and Table (1). The particles size analyses showed that the dust

consist of very fine aggregates of particles (Table 1). It was found that, 50 % of dust particles below (1.63 - 3.15 μm), while the majority of particles (> 90 %) below (5.42 - 7.07 μm). The results indicated that, ferrochrome converter (CRC) dust has particles coarser than the dusts generated from electric arc furnace (EAFSS & EAFCS). The median particle size for CRC is 3.15 μm , while the median particle size for EAFSS and EAFCS are 2.37 and 1.63 μm , respectively (Table1).

From the granulometric analyses results, the physical separation techniques such as magnetic, gravity and flotation, are not suitable to treat these materials. Most dust particles fall below 5 μm , such fine particles are very difficult to beneficiate via conventional mineral processing processes [15]. In addition to, the very fine grained distribution of steel dusts makes these materials difficult to handle dry, and can be easily be airborne if no previous agglomeration is used [16]. The results of particle size distribution are in agreement with the results obtained by other researchers [16-17]. They concluded that EAF dusts consist of very fine particles with almost 90% of the particles are lower than 10 μm and the metals are more concentrated in the fine fraction of the waste [16 - 17].

4.2. Mineralogical composition

The identified phases in the CRC, EAFSS and EAFCS dusts, according to qualitative phase analysis, are shown in Fig. (6).

The main elements in the dusts are iron, zinc and chromium mostly presented as complex oxides with spinel structure. From the XRD pattern, peaks like the peaks of chromite (FeCr_2O_4), magnetite (Fe_3O_4) and franklinite (ZnFe_2O_4) have been identified in the XRD pattern. The peaks from these phases exhibit overlapping in some extent, as shown in Fig. 6. Because of such overlapping, the presence of these phases cannot be unequivocally assured. Consequently, it was impossible to identify these phases by XRD, SEM coupled with EDS used for identification of these phases. In addition to spinel group phases, zincite (ZnO), portlandite $\text{Ca}(\text{OH})_2$, lime (CaO) and periclase (MgO) have been identified. Lime and MgO particles have been caught by the gas flow when lime

has been charged into the CRC and EAF. The main phases identified in the dusts are consistent with the results obtained by previous study [3, 6].

4.3. Chemical composition

The chemical composition of the three representative dust samples used in this study are shown in Table (2). The moisture contents of all dust samples are low (<1 wt.%). The pH values in the range from 10 to 11 which indicated that the dusts are basic.

A comparison between the chemical analyses of steelmaking dusts from different origins reveals a significant variation in the elemental composition. The chemical composition of the dust depends on the batch feed material and the operating parameters of furnace or converter during production [18, 4]. The results showed that, the dusts from carbon steelmaking (EAFCS) are rich in zinc, while the dusts from stainless steelmaking (CRC & EAFSS) are relatively low in zinc, but richer in chromium. Previous investigation stated that, the zinc content in carbon steel dust is typically from 15 to 35 wt.%, which is generally much higher than in dusts generated in stainless steel production [18, 4]. The contents of zinc (Zn) in CRC, EAFSS and EAFCS dusts are 10.83, 19.84, and 35.76 wt.%, respectively, while the contents of chromium (Cr) are 20.88, 3.19 and 0.47 wt.%, respectively (Table 2). It's obvious that CRC dust contains high amount of chromium compared to the electric arc furnace dust. This due to that, the feed material to the chromium converter is liquid ferrochrome, which produce in the same location from chromite ore by using submerged arc furnaces (SAF). In addition to iron, zinc and chromium the dusts are characterized by relatively high contents of calcium oxide and magnesium oxide, due to the dolomitic lime added to the steelmaking furnace [6]. The CaO contents in CRC, EAFSS and EAFCS dusts are 14.27, 11.91 and 5.93 wt.%, respectively (Table 2).

The concentration of Pb, Cl, S and alkaline elements (such as K) in carbon steel dust is higher than in the dust from stainless steel. It was reported that carbon steel dust is rich in lead than the dusts

generated from stainless steel production [18, 4]. The lead comes from the paint present in the scrap pieces [6]. The Pb contents in CRC, EAFSS and EAFCS dusts are 0.11, 0.62 and 2.15 wt. %, respectively (Table 2).

Distributions of trace elements in the dusts are listed in Table 2. V, Ba, Ga, Ta, Sr, Sn, Sb, Rb, Zr and Cs records the highest concentrations in the dusts. Other elements exhibit relatively low concentrations (below 38 ppm). Ferrochrome converter (CRC) dust has higher V, Ga and Ta contents in the range of 426, 375 and 191 ppm, respectively. EAFSS dust contains high amount of Ba and Mo in the range of 745 and 586 ppm, respectively. EAFCS dust has high contents of Ta, Ba and Sn in the range of 434, 433 and 234 ppm, respectively (Table 2).

4.4. Microstructure of steelmaking dusts

The microstructure and microanalyses of the particles of the dusts were obtained by means of SEM-EDS.

Fig. (7) shows SEM images of ferrochrome converter (CRC) dust, and Table (3) gives the microanalyses of the phases of CRC dust in Fig. (7). The general distribution of CRC dust particles is shown in Fig. (7A), particles are occurring as irregular particles of chromite. In addition to fine grained of periclase (MgO), portlandite Ca(OH)_2 and zincite spheres. Fig. (7B) shows that there are angular phases enclosed in calcium-iron-silicate glass spheres, the angular phases are magnesiochromite (Fe, Mg) Cr_2O_4 . EDS analyses (Table 3, S1-4) demonstrate that there are magnesiochromite crystals enclosed in calcium silicate glass sphere. Chromite particles of irregular shape were detected (Fig.7 C&D – S5-7), these particles are probably originate from chromite raw material which used in SAF. Fig. 7C shows large chromite fragment covered with fine grained material of different composition with spinel structure of Ca-Si-Cr-Fe-O (Fig. 7D). Small particles of different shape were observed in the dusts (Fig. 7E&F – S8-12). These grains are composed of Fe-Cr, C-O, Fe-O and Si-Cr-Fe-O, probably a variation of ferrochrome, coke, magnetite and Si rich chromite, respectively (Table 3 – S8-12). Zincite sphere of monocrystal with size lower than 2 μm

was detected in the dust (Fig. 7F – Table 3 S14-15). These zincite sphere forms during the condensation of the vapors of zinc contained in the fumes [14]. Figs. (7G&H) show there are agglomeration of fine grained of MgO and CaO oxide, which related to periclase, lime and portlandite as indicated with XRD. Close up figure (Fig. 7H) showed that, there are white spheres of CaO particles are dispersed in MgO fine grained materials, as indicated with EDS (Table 3 – S16-19). These particles are originated from fluxes added in the steelmaking process [6]. Makkonen *et.al.* [12] indicated that the non-spherical form and different phase composition of CRC dust is similar to FeCr slag from the submerged arc furnace (SAF) in the ferrochrome plant. Because with molten ferrochrome from the ferrochrome plant, some FeCr slag from the SAF has been introduced into the CRC and a particle of the slag has ended up in the CRC dust.

Electric arc furnace stainless steel (EAFSS) dust is characterized by encapsulation phenomenon (Figs. 8A-D). The microanalyses of the phases of EAFSS dust are presented in Table (4). Figs. (8A-C) show that the encapsulation particles are often surrounded by fine-grained particles and spheres. From the general distribution of EAFSS dust particles, large particles of dust $> 3 \mu\text{m}$ are characterized by encapsulation phenomenon. Fig. (8A – 8C) and (Table 4 S1-11) show that franklinite phases are enclosed in calcium-iron-silicate glass spheres. Fig. (8B – Table 4 S5-6) shows that aggregates of franklinite enclosed in a glass sphere. Occasionally, small grains have agglomerated and formed larger particles (Fig. 8B). Fig. (8C) and (Table 4 S10-11) shown that franklinite particles of different shapes are enclosed in glass spheres. EDS analyses indicated that franklinite particles are rich in Manganese (Mn) (Table 4). The correlation between Mn and Zn concentrations in EAFSS dust particles indicated that, Mn show high concentration in franklinite particles (Table 4). Fig. (9A) show that Mn exhibit positive correlation ($r^2 = 0.72$) with Zn, manifesting that Mn and Zn belong to the same phase, franklinite $(\text{Zn}, \text{Mn}^{+2}, \text{Fe}^{+2})(\text{Fe}^{+3}, \text{Mn}^{+3})_2 \text{O}_4$. Figure (8D) and Table (4 – S12-13) shown that there are angular phases enclosed in calcium-iron-silicate glass sphere, the angular phases are chromite (FeCr_2O_4). Chromite particles are rich in

nickel, the content of Ni was 9.55 wt.%. While the content of Cr is 37 wt.%, which indicate that nickel are present in the structure of the chromite. On the other hand, the fine particle $< 1 \mu\text{m}$ of EAFSS dust is characterized by spherical form and fragments of irregular shape. Franklinite spheres and fragments was detected in the fine particles (Fig.8 – S3, S8). Spheres of particles with spinel structure, rich in zinc and iron and particles rich in zinc, manganese, iron and magnesium were detected (Fig. 8A,B and F) and (Table 4 – S3, S8 and S18). Also fragments of chromite (Fig. 8E – S15) and magnetite (Fig. 8 – S9, S14 and S17) were detected in the EAFSS dust. Particles of magnesium oxide were detected in the EAFSS dust (Fig. 8F – S16). SEM investigation indicated that in the larger particles of EAFSS dust, franklinite and chromite crystals are enclosed in the glass sphere, but in the fine-grained fraction of the dust, no similar encapsulation phenomenon was observed. This encapsulation phenomenon will influence the leaching of zinc and chromium, because the enveloping glass must be dissolved before the phases with high Zn and Cr contents can be leached [12].

The electric arc furnace carbon steel (EAFCS) dust is dominated by spherical form, which indicates the formation by ejection from the liquid metal. This characterized spherical morphology has been detected by other researchers [3, 8]. The general distribution of EAFCS dust particles are shown in Figs. (10A&B), and the microanalyses of the phases present in EAFCS dust are listed in Table (5). EDS analyses revealed that the spherical particles rich in Fe, Zn and O as major elements were assigned to franklinite (Fig. 10A – Table 5 S1-4). The chemical analyses of different franklinite particles indicated that, franklinite is rich in Manganese (Mn). The contents of Mn in the franklinite particles are in the range of 4 -10 wt.%, which suggested that manganese is present in the structure of franklinite or present as fine particles attached to franklinite spheres. Fig. (9B) showed that, Mn concentrations show positive correlation ($r^2 = 0.67$) with Zn, demonstrating that Mn and Zn belong to the same phase, franklinite $(\text{Zn}, \text{Mn}^{+2}, \text{Fe}^{+2}) (\text{Fe}^{+3}, \text{Mn}^{+3})_2 \text{O}_4$. Zincite spheres were identified in the EAFCS dust (Fig. 10B- S5-8), the size of zincite spheres are lower than $1 \mu\text{m}$. The Zn content in the

analyses particles was 68.49 wt.% and the content of Fe was 3.45 wt.%, the high Zn content and the low Fe content indicate that the grain is zincite than zinc ferrite (Table 5). The zincite is also detected by XRD.

In addition to the main spherical form of the EAFCS particles, there are franklinite particles of different shape were observed (Fig. 10C and D). Fig. (Fig. 10C) shows that smaller franklinite particles agglomerated together to form large particle. Fig. (Fig. 10D – S10-11) shows that there are franklinite phases enclosed in calcium-iron-silicate glass spheres, the Zn content in the franklinite particles are much higher than in the surrounding glass. Also smaller particles of irregular shape of franklinite ($< 1\mu\text{m}$) were detected (Fig. 10D and F – S12, S17). Franklinite with fibers crystals also detected (Fig. 10F- S18), EDS analysis indicated that these fibers particles contain 2.36 % Pb. An irregular and porous particles of magnetite (Fe_3O_4) were detected in EAFCS dust (Fig.10 E and F – S13-16). Some magnetite particles show signs of melting, and formed from agglomeration of small particles (Fig.10 G – S19). Large particle of irregular shape of Si-O-Al was found (Fig.10 H – S20). Probably, it is a phase rich in magnesium, silicon and calcium originated from fluxes added in the steelmaking process.

4.5. Fourier transform Infrared (FTIR) spectroscopy

The FTIR spectrums of CRC, EAFSS and EAFCS dusts are shown in Fig. (11). In all samples, the sharp band that appears at 3640 cm^{-1} can be assigned to hydroxyl stretching modes. This band confirms the presence of hydroxides in the dusts and corresponds to hydroxyl stretching vibrations of calcium hydroxide [19]. XRD analyses detected portlandite $\text{Ca}(\text{OH})_2$ phase in the samples. In EAFSS dust a tiny band at 3569 cm^{-1} has been detected, this band related to hydroxyl stretching modes of hydrated aluminum compounds [19, 20]. XRF analyses indicated that EAFSS dust contains about 1 % of Al oxide. In both CRC and EAFSS dusts the band at 1623 cm^{-1} is due to the OH bending of water and hydrated phases present in the dusts [19]. The bands located at 626, 582, 592, 541, 440 and 465 cm^{-1} are a common feature of simple metal oxides (like, ZnO) and complex

spinel group (AB_2O_4) [21]. The spinel phases found in the dusts include franklinite ($ZnFe_2O_4$), magnetite (Fe_3O_4) and chromite ($CrFe_2O_4$). Due to the bands overlap of the different constituents in this region of the spectrum, it is very difficult to obtain detailed structural information [19]. The spinel group compounds have been identified by using couple SEM and EDX techniques. In both EAFSS and EAFCS dusts, the spectra positioned at 2860, 2925 and 2960 cm^{-1} are assigned to C-H stretch of aliphatic carbon chain indicating the presence of organic matter [6]. The bands in the region from 1106 to 1141 cm^{-1} are assigned to Si-O vibrations [22]. In the spectrum of EAFCS dust the band located around 1199 cm^{-1} is due to a sulphate (SO_4^{2-}) vibration, the band at 626 cm^{-1} also assigned to sulphate vibration [6]. The band at 626 cm^{-1} is overlap with the vibration band of spinel group. In all samples the bands that appear at 1797 and 1417 cm^{-1} correspond to C-O stretching modes of the carbonate CO_3^{2-} ion, the bands at 715 and 707 cm^{-1} can be assigned to deformation modes of the C-O vibrations [23].

4.6. Thermoanalyses

Differential scanning calorimetry (DSC) and Thermogravimetry (TG) combined with Mass spectra (MS) spectroscopy were used to study the thermal behaviour of CRC, EAFSS and EAFCS dusts. The results of thermoanalyses are shown in Figs. (12-14).

The DSC-TG curves indicated that, CRC, EAFSS and EAFCS dusts have a similar thermal behavior in the temperature range below 800 °C, but above this range there are apparent differences in their thermal behavior. In the temperature range below 800 °C, the first peak occurred in the range of 190 °C, with less weight loss (about 0.5% of the total weight), this reaction corresponding to the evaporation of physically adsorbed water (Figs. 12-14). There are two distinct stages of reactions at 400-450 and 560-650, associated with weight loss TG curve (Figs. 12-14). These reactions are related to the dehydroxylation of calcium hydroxide and the decomposition of calcium carbonate, respectively, according to the following reactions.



Mass spectra curves indicated that the evolution of H_2O and CO_2 from the sample at these temperature ranges (Figs.12-14). The result is consistent with the results obtained by other researchers [5, 19, 24, 25]. The weight loss in the two reactions in the CRC, EAFSS and EAFCS dusts are (0.92 – 0.82 %), (0.37 -0.70 %) and (0.17 – 1.42 %), respectively. The weight loss in CRC dust is higher than EAFSS and EAFCS dusts, which indicated that CRC dust contains higher Ca(OH)_2 and CaCO_3 than EAFSS and EAFCS dusts. Both Ca(OH)_2 and CaCO_3 are existing originally in the dusts as free lime which, in turn, may have hydrated and carbonated on exposure to ambient moisture and CO_2 for extended periods of time [19]. There are weak reactions occurring in the temperature range of 500 °C connected with a slight weight gain < 0.5 % (Figs. 12-14). This may be due to the oxidation of some free iron oxide to a higher oxidation state [24].

In the temperature above 800 °C, Figs. (12-14) show that there are apparent differences in the mass loss of the dust samples, although there are no corresponding gases release detected by MS or thermal reactions observed with DSC. This phenomena was observed by other studies [5, 24], and related to the volatilization of condensable chlorides of Zn, Pb and K. Mikhail *et al.* [24] found that a white precipitate of PbCl , NaCl and KCl has been found deposited on the reaction tube after heating steel dust sample to 1000 °C. CRC dust shows slight weight loss < 0.5 %, this may be due to that CRC dust contain less volatile elements (0.11 wt.% Pb, 0.29 wt.% Cl, 0.74 wt.% K_2O), in addition to low carbon content < 0.3 wt.%. The carbon contained in the dust can react with zinc, which evaporated into zinc vapour. On the other hand, EAFSS and EAFCS dusts show higher weight loss of 4.8 and 8.3 %, respectively, due to the high contents of Pb, Cl, K and C in these dusts. EAFSS dust contains (0.62 wt.% Pb, 1.25 wt.% Cl, 1.49 wt.% K_2O and 0.5 wt.% C), while EAFCS dust contains (2.15 wt.% Pb, 1.69 wt.% Cl, 3.21 wt.% K_2O and 1.5 wt.% C). There are endothermic peaks at 1260 °C which related to the decomposition of unfused calcium carbonate [26].

5. Implications of present study for utilization of steelmaking dust

The direct recycling of steelmaking dust back to the blast furnace and electric arc furnace through direct charging of briquettes or micro-pellets, is economically viable [27, 28]. The main obstacle associated with recycling the dust back to the furnace is the high content of zinc and volatile components [29]. Volatile components cause problems when charged to a furnace, which affect the refractory materials, and thus decrease the productivities. Therefore, how to separate zinc from the steelmaking dusts in an economic way becomes a crucial step for recycling of these wastes in iron and steelmaking industry [30]. There are two main processes for zinc recovery include hydrometallurgical [5, 31, 32] and pyrometallurgical methods [33-35]. The choice between the two methods strongly depends on the properties of materials [16]. The factors which determine the suitable processing method are: the mineralogical composition of dust, zinc form (zinc oxide or zinc ferrite), concentration of zinc and alkali elements, and microstructure of particles. Therefore, before choosing the processing method, a detailed characterization of dust is an essential step in determining the most appropriate recycling strategy [16].

In the present study, the determination of concentration and mode of zinc occurrence in the steelmaking dust can help to design the suitable process for utilizing these waste in steel making industries again. In the dusts from EAFSS and EAFCS, the results indicated that hydrometallurgical methods are not effective to remove zinc from these dusts, because zinc mostly exists in the zinc ferrite phase which is quite stable and insoluble in most acidic and alkaline solutions [36]. SEM-EDX investigation revealed that EAFSS dust are dominated with encapsulation particles, franklinite crystals are enclosed in a glass sphere. This encapsulation phenomenon will influence the leaching of zinc, because the enveloping glass must be dissolved before the phases with high Zn contents can be leached. For these reasons, pyrometallurgical methods are more suitable for processing EAFSS

and EAFCS dusts. On the other hand, ferrochrome converter (CRC) dust is characterized by high chromium content (20.88 wt.%) and low zinc content (10.80 wt.%). In addition, the zinc occurs as zinc oxide, which does not cause problems in hydrometallurgical treatment. Therefore, the low zinc content and the existing of zinc in zincite phase leads to greater interest in the hydrometallurgical methods than pyrometallurgical methods [37]. Makkonen *et.al.* [12] studied the leaching of ferrochrome converter (CRC) dust from Outokumpu Tornio Plant, Finland with a sulfuric acid solution. The authors [12] concluded that the highest Zn dissolution ratio (94 %) is due to the existence of zinc in the zincite phase.

Recently, many researchers have begun to pay attention to microwave energy as an alternative recycling method [38 -42]. Instead of conventional heating, microwave heating is exploited, which gives different heat transfer and mass transfer mechanisms. In the second part of this work, microwave heating technology will be utilized to handle steelmaking dusts. The main advantages of microwave treatment of steelmaking dusts are: (1) Microwaves can heat zinc ferrite in the steelmaking dust quickly and efficiently. (2) Microwaves can reduce zinc ferrite to iron and zinc metals, instead of zinc oxide in conventional heating processes [38]. (3) Higher reaction rates can be obtained by microwave [39]. (4) Microwave heating does not require any pretreatment (e.g. injection of gas), which makes it possible to use fine particles directly [42].

Conclusions:

Detailed characterization of steelmaking dusts from Finnish steelmaking plants with several analytical techniques was carried out in order to get essential information for developing the recycling methods for these wastes. The results showed that steelmaking dusts from CRC, EAFSS, and EAFCS show significant difference in concentration and mode of occurrence of zinc in the dusts, which will influence on determine treatment methods. In the EAFSS and EAFCS dusts, zinc mainly exists in the zinc ferrite phase and dominated by encapsulation phenomenon, franklinite crystals are enclosed in a calcium-iron-silicate glass sphere. Based on these observations, hydrometallurgical methods are not effective to remove zinc from EAFSS and EAFCS dusts. The encapsulation particles will influence on the leaching of zinc, in addition to zinc ferrite phase which is refractory against leaching. Therefore, pyrometallurgical methods will be more suitable for processing EAFSS and EAFCS dusts. On the other hand, CRC dust has low zinc content, and the zinc occurs as zinc oxide sphere. The low zinc content and the presence of zinc in zincite phase leads to greater interest in the hydrometallurgical methods than pyrometallurgical methods.

Acknowledgement:

The authors would like to thank Mr. Niko Hyttinen from Outokumpu Tornio plant, and Mrs. Helena Erkkilä, Mr. Ville Fomkin and Mr. Kari Välimaa from Ovako Imatra, Finland, for the discussions and for their offers of industrial samples. The authors thank Mr. Riku Mattila and Mr. Tommi Kokkonen for their technical support throughout this work. The authors are indebted to Mr. Ari Väliheikki for help in FTIR analyses, Mrs. Leena Palmu for the XRF analyses and Mr. Jarno Karvonen for granulometric analyses.

References

- [1] Z. Huaiwei, H. Xin, An overview for the utilization of wastes from stainless steel industries, *Resour. Conserv. Recycl.* 55 (2011) 745-754.
- [2] B. Das, S. Prakash, P.S.R. Reddy, V.N. Misra, An overview of utilization of slag and sludge from steel industries, *Resour. Conserv. Recycl.* 50 (2007) 40-57.
- [3] J.G.M.S. Machado, F.A. Brehm, C. A.M. Moraes, C.A. dos Santos, A.C.F. Vilela, J.B.M. da Cunha, Chemical, physical, structural and morphological characterization of the electric arc furnace dust, *J. Hazard. Mater.* B136 (2006) 953-960.
- [4] D.K. Xia, C.A. Pickles, Microwave caustic leaching of electric arc furnace dust, *Miner. Engin.* 13 (2000) 79-94.
- [5] P. Oustadakis, P.E. Tsakiridis, A. Katsiapi, S. Agatzini-Leonardou, Hydrometallurgical process for zinc recovery from electric arc furnace dust (EAFD) Part I: Characterization and leaching by diluted sulphuric acid, *J. Hazard. Mater.* 179 (2010) 1-7.
- [6] F.M. Martins, J.M.R. Neto, C.J. Cunha, Mineral phases of weathered and recent electric arc furnace dust, *J. Hazard. Mater.* 154 (2008) 417-425.
- [7] T. Sofilić, A. Rastovčan-Mioč, Š. Cerjan-Stefanović, V. Novosel-Radović, M. Jenko, Characterization of steel mill electric-arc furnace dust, *J. Hazard. Mater.* 109 (2004) 59-70.
- [8] G. Orhan, Leaching and cementation of heavy metals from electric arc furnace dust in alkaline medium. *Hydrometallurgy* 78 (2005) 236-245.
- [9] G. Salihoglu, V. Pinarli, Steel foundry electric arc furnace dust management: stabilization by using lime and Portland cement, *J. Hazard. Mater.* 153 (2008) 1110-1116.
- [10] C.F. Pereira, Y.L. Galiano, M.A. Rodriguez-Piñero, J.V. Parapar, Long and short term performance of a stabilized/solidified electric arc furnace dust. *J. Hazard. Mater.* 148 (2007) 701-707.
- [11] E-P. Heikkinen, On the Role of Computational Thermodynamics in Research and Development of AOD and CRC processes, Doctoral Thesis, University of Oulu, 2013.
- [12] H. T. Makkonen, A. Kekki, E-P. Heikkinen, T. Fabritius, J. Aromaa, O. Forsen, Characterization and Sulfuric Acid Leaching of Ferrochrome Converter (CRC) Dust, *steel research int.* 86 (2015) 1-9.

- [13] E-P. Heikkinen, T. Fabritius, Modelling of the Refining Processes in the Production of Ferrochrome and Stainless Steel. In: Nusheh, M., Ahuett, G.H., Arrambide, A. (eds.). Recent Researches in Metallurgical Engineering - From Extraction to Forming, In Tech. 186 (2012) 65-88.
- [14] A-G. Guèzennec, J-Ch. Huber, F. Patisson, Ph. Sessiecq, J-P. Birat, D. Ablitzer, Dust formation in Electric Arc Furnace: Birth of the particles, Powder Technol. 157 (2005) 2-11.
- [15] H. Shen, E. Forssberg, U. Nordström, Physicochemical and mineralogical properties of stainless steel slags oriented to metal recovery, Resour. Conserv. Recycl. 40 (2004) 245–271.
- [16] A.J.B. Dutra, P.R.P. Paiva, L.M. Tavares, Alkaline leaching of zinc from electric arc furnace steel dust, Miner. Engin. 19 (2006) 478-485.
- [17] N. Menad, J.N. Ayala, F.G. Carcedo, E.R. Ayúcar, A. Hernández, Study of the presence of fluorine in the recycled fractions during carbothermal treatment of EAF dust, Waste Manag. (2003) 483-491.
- [18] T. Havlik, B.V. Souza, A.M. Bernardes, I.A.H. Schneider, A. Miskufova, Hydrometallurgical processing of carbon steel EAF dust, J. Hazard. Mater. B135 (2006) 311-318.
- [19] C. Navarro, M. Díaz, M. Villa-García, Physico-Chemical Characterization of Steel Slag. Study of its Behavior under Simulated Environmental Conditions, Environ. Sci. Technol. 44 (2010) 5383-5388.
- [20] R.L. Frost, J. Klopogge, S. C. Rusell, J. L. Szetu, Dehydroxylation and structure of alumina gels prepared from trisecbutoxyaluminium, Thermochim. Acta. 329 (1999) 47-56.
- [21] G.C. Allen, M. Paul, Chemical characterization of transition metal spinel type oxides by infrared spectroscopy, Appl. Spectrosc. 49 (1995) 451-458.
- [22] M.J. Wilson, Clay Mineralogy: Spectroscopic and Chemical Determinative Methods, first ed., Chapman & Hall, London, 1994.
- [23] D.W. Mayo, A.M. Foil, R.W. Hannah, Course Notes on the Interpretation of Infrared and Raman Spectra. Wiley-Interscience: New York, (2004) 316-318.
- [24] S.A. Mikhail, A-M. Turcotte, Thermal reduction of steel-making secondary materials I. Basic-oxygen-furnace dust, Thermochimica Acta 311 (1998) 113-119.
- [25] S.A. Mikhail, A-M. Turcotte, J. Aota, Thermoanalytical study of EAF dust and its vitrification product, Thermochim. Acta. 287 (1996) 71-79.
- [26] I.D. Kashcheev, E.A. Terentév, K.N. Demidov, T.V. Borisova, I.D. Maryasev, Properties and structure of magnesia modifiers for converter slags, Refract. Ind. Ceram. 48 (1) (2007) 17-22.
- [27] K. Wu, T. Yang, H.W. Gudenau, Treatment of recycling fine dust formed in ironmaking and steelmaking processes with injecting method, Iron and Steel. 34 (1999) 60-66.

- [28] H.W. Gudenau, K. Stoesser, H. Denecke, V. Schemann, Environmental aspects and recycling of filter dusts by direct injection or use of agglomerates in shaft furnaces, *ISIJ Int.* 40 (2000) 218-223.
- [29] H.T. Makkonen, J. Heino, L. Laitila, A. Hiltunen, E. Pöyliö, J. Härkki, Optimisation of steel plant recycling in Finland: dusts, scales and sludge, *Resour. Conserv. Recycl.* 35 (2002) 77-84.
- [30] N. Ma, Recycling of basic oxygen furnace steelmaking dust by in-process separation of zinc from the dust, *J. Cleaner Product.* 112 (2016) 4497-4504.
- [31] T. Miki, R. Chairaksa-Fujimoto, K. Maruyama, T. Nagasaka, Hydrometallurgical extraction of zinc from CaO treated EAF dust in ammonium chloride solution, *J. Hazard. Mater.* 302 (2016) 90-96.
- [32] M. Al-harashsheh, S. Kingmanb, L. Al-Makhadmah, I.E. Hamilton, Microwave treatment of electric arc furnace dust with PVC: Dielectric characterization and pyrolysis-leaching, *J. Hazard. Mater.* 274 (2014) 87-97.
- [33] J.A. de Araújo, V. Schalch, Recycling of electric arc furnace (EAF) dust for use in steel making process, *J. Mater. Research Technol.* 3(3) (2014) 274-279.
- [34] E. Kim, T. Kim, J. Lee, Y. Kang, K. Morita, Reduction of electric arc furnace dust by graphite powders under microwave irradiation, *Ironmak. Steelmak.* 39:1 (2012) 45-50.
- [35] M.C. Mantovani, C. Takano, The strength and the high temperature behaviour of self-reducing pellets containing EAF dust, *ISIJ Int.* 40(3) (2000) 224-230.
- [36] F. Elgersma, G.F. Kamst, G.J. Witkamp, G.M. Van Rosmalen, Acidic dissolution of zinc ferrite, *Hydrometallurgy*, 29 (1992) 173-189.
- [37] R.L. Nyirenda, The processing of steelmaking flue-dust: a review, *Miner. Engin.* 4 (7-11) (1991) 1003-1025.
- [38] X. Sun, J-Y. Hwang, X. Huang, The Microwave Processing of Electric Arc Furnace Dust, *JOM*, 60(10) (2008) 35-39.
- [39] J. Vereš, M. Lovás, Š. Jakabský, V. Šepelák, S. Hredzák, Characterization of blast furnace sludge and removal of zinc by microwave assisted extraction, *Hydrometallurgy* 129-130 (2012) 67-73.
- [40] K. Nishioka, T. Maeda, M. Shimizu, Dezincing behaviour from iron and steelmaking dusts by microwave heating, *ISIJ Int.* 42 (2002) S19-S22.
- [41] S. Cho, J. Lee, Metal Recovery from Stainless Steel Mill Scale by Microwave Heating. *Metals Mater. Int.* 14 (2) (2008) 193-196.
- [42] M.B. Mourao, Jr. Parreiras de Carvalho, C. Takano, Carbothermic Reduction by Microwave Heating, *ISIJ Int.* 41 (2001) S27-S30.

List of figures

Fig. 1: The flow sheet for the production processes in Outokumpu Stainless and Outokumpu Chrome Tornio, Finland.

Fig. 2: The flow sheet for the production processes in Ovako Imatra, Finland.

Fig. 3: Particle size distribution of CRC dust.

Fig. 4: Particle size distribution of EAFSS dust.

Fig. 5: Particle size distribution of EAFCS dust.

Fig. 6: X-ray diffraction (XRD) pattern of CRC, EAFSS, and EAFCS dusts.

- | | |
|--|---|
| 1. Magnetite (Fe_3O_4) (DB: 04-001-7822) | 5. Lime (CaO) (DB: 04-003-7161) |
| 2. Franklinite (ZnFe_2O_4) (DB: 04-009-8433) | 6. Periclase (MgO) (DB: 04-001-7295) |
| 3. Chromite (FeCr_2O_4) (DB: 01-082-3028) | 7. Portlandite ($\text{Ca}(\text{OH})_2$) (DB: 04-010-3117) |
| 4. Zincite (ZnO) (DB: 04-005-4711) | |

Fig. 7: (A) SEM photomicrographs shows the distribution of CRC dust particles. (B) Mg-chromite crystals (S1&S2) enclosed in calcium–iron–silicate glass (S3&S4). (C) Chromite particles of irregular shape (S5&S6). (D) A close up to chromite fragment (S7), shows that chromite particle covered with fine grained material of different composition of Ca-Si-Cr-Fe-O (Red arrow). (E) Irregular particles of Fe-Cr (S8), coke (S9) and Magnetite (S10). (F) Zincite sphere of monocrystal (S14&S15). (G) Agglomeration from CaO (S16) and MgO (S17) fine grained material. (H) Close up figure shows that, white spheres of portlandite (S18) are dispersed in MgO (S19) fine grained materials.

Fig. 8: (A-C) SEM photomicrographs show the general distribution of EAFSS dust particles, large particles $> 3 \mu\text{m}$ are characterized by encapsulation phenomenon and surrounded by fine-grained particles. **(A)** Franklinite phase (S2) enclosed in glass sphere (S1). **(B)** Aggregates of franklinite crystals (S5-S8) enclosed in glass sphere. **(C)** Franklinite particles (S10) are enclosed in glass sphere (S11). **(D)** Ni chromite crystals (S12) enclosed in the calcium-iron-silicate glass spheres (S13). **(E)** Magnetite particle (S14) and fragments of chromite (S15). **(F)** Periclase (S16) particle.

Fig. 9: Positive correlations between manganese (Mn) and zinc (Zn) concentrations in EAFSS (A), and EAFCS (B).

Fig. 10: (A&B) SEM photomicrographs show the general distribution of EAFCS dust particles are dominated with spherical form. **(A)** SEM photomicrographs show franklinite spheres (S1-S4). **(B)** SEM photomicrographs show zincite spheres (S6-S8). **(C)** Smaller franklinite particles (S9) agglomerated together to form large particle. **(D)** Franklinite phases (S10) enclosed in calcium-iron-silicate glass spheres (S11). **(E)** Irregular particles of magnetite (S13-S15). **(F)** Fibers crystals of franklinite rich in Pb (S18). **(G)** Large and porous magnetite particle show sign of melting (S19). **(H)** Large particle of irregular shape of Si-O-Al (S20).

Fig. 11: FT-IR spectra for CRC, EAFSS, and EAFCS dusts.

Fig. 12: TG-DSC curves and mass spectrometry curves for CRC dust.

Fig. 13: TG-DSC curves and mass spectrometry curves for EAFSS dust.

Fig. 14: TG-DSC curves and mass spectrometry curves for EAFCS dust.

Table (1). Granularity analyses of ferrochrome converter (CRC), electric arc furnace stainless steel (EAFSS), and electric arc furnace carbon steel (EAFCS) dusts.

	CRC	EAFSS	EAFCS
	Particle size (μm)		
d_{10}	0.17	0.13	0.18
d_{25}	0.84	0.31	0.48
d_{50}	3.15	2.37	1.63
d_{75}	4.84	3.94	2.96
d_{90}	7.07	6.26	5.42
d_{100}	15.42	13.00	14.62
Median (d_{50})	3.15	2.37	1.63
Mean	3.56	2.87	2.46
Mode	3.68	3.05	2.31
Skewness	1.57	1.62	2.47
Kurtosis	3.45	2.90	6.71

Table (2). Chemical composition of ferrochrome converter (CRC), electric arc furnace stainless steel (EAFSS), and electric arc furnace carbon steel (EAFCS) dusts.

	CRC	EAFSS	EAFCS	Analysing method		CRC	EAFSS	EAFCS
Elements	Major elements (wt.%)				Elements	Minor elements (ppm)		
C	0.3	0.5	1.5	LECO	V	426	117	121
Fe	18.74	23.70	23.50	XRF	Ga	375	370	184
Zn	10.83	19.84	35.76	XRF	Ba	129	745	431
Cr	20.88	3.19	0.47	XRF	Ta	191	301	433
CaO	14.27	11.91	5.93	XRF	Mo	21	586	79
MgO	9.76	7.21	1.07	XRF	Sn	44	325	234
MnO	1.56	5.82	3.99	XRF	Sr	41	193	58
SiO ₂	9.99	8.75	3.13	XRF	Rb	22	49	103
K ₂ O	0.74	1.49	3.21	XRF	Sb	38	80	94
Al ₂ O ₃	0.80	0.87	0.27	XRF	Cs	0	5	191
Cl	0.29	1.25	1.69	XRF	Nd	0	33	78
F	0.31	0.51	0.37	XRF	U	4	19	58
P ₂ O ₅	0.02	0.08	0.13	XRF	Ge	0	0	39
S	0.14	0.48	1.22	XRF	Zr	17	19	45
TiO ₂	0.09	0.09	0.05	XRF	Bi	4	40	0
Pb	0.11	0.62	2.15	XRF	Nb	0	25	0
Ni	0.25	0.37	0.038	XRF	Sc	4	4	4
Cu	0.032	0.30	0.25	XRF	La	10	10	10
					Pr	10	5	5
pH	10	10-11	10-11		As	13	0	0
Moisture %	0.22	0.30	0.54		Hf	6	9	16
					Th	2	2	2

Table (3). Microanalyses of the phases of ferrochrome converter (CRC) in Figure (7).

[illegible]

Table (5). Microanalyses of the phases of electric arc furnace carbon steel (EAFCS) in Figure (10).

[illegible]

Figure 1

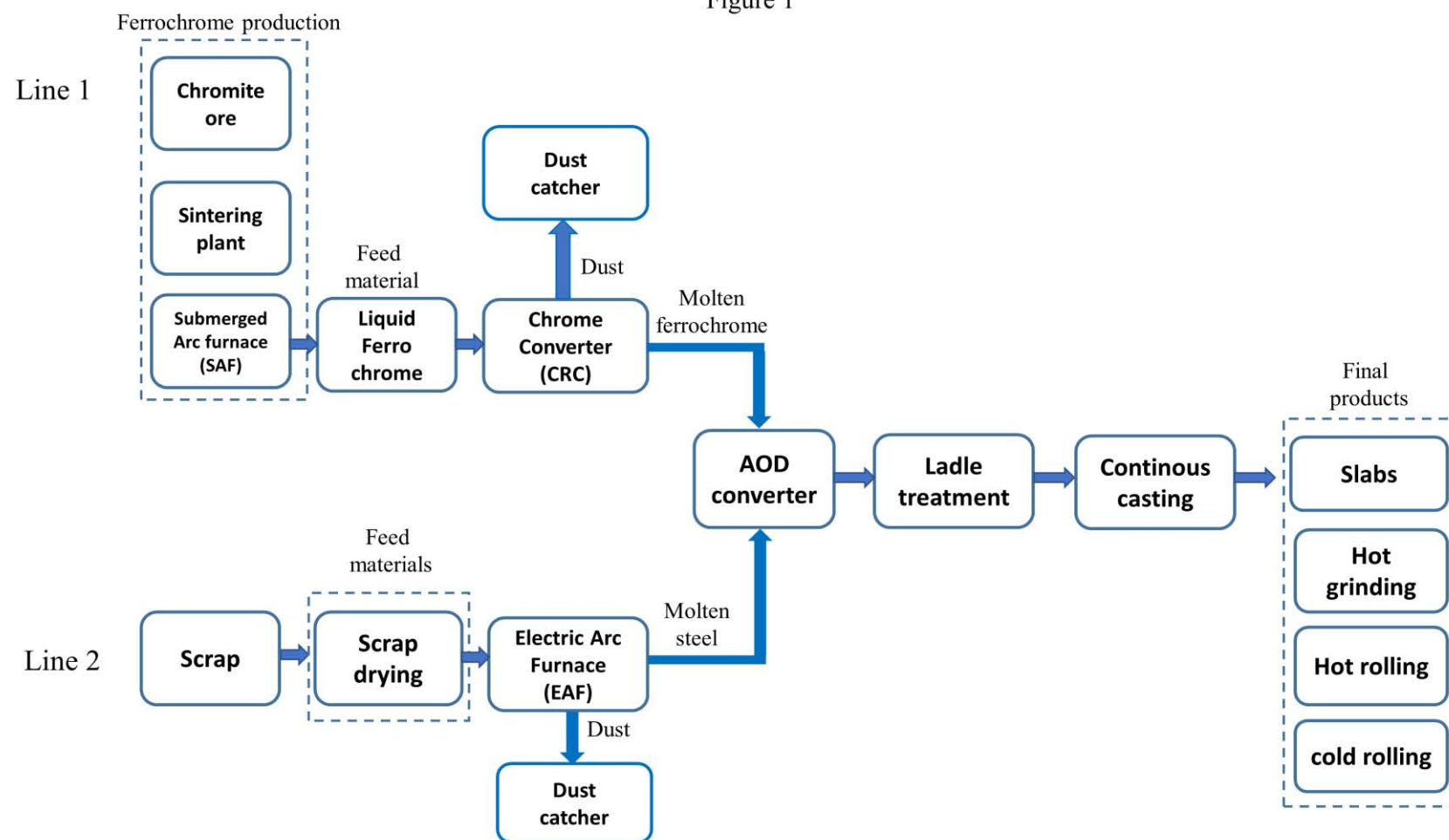


Figure 2

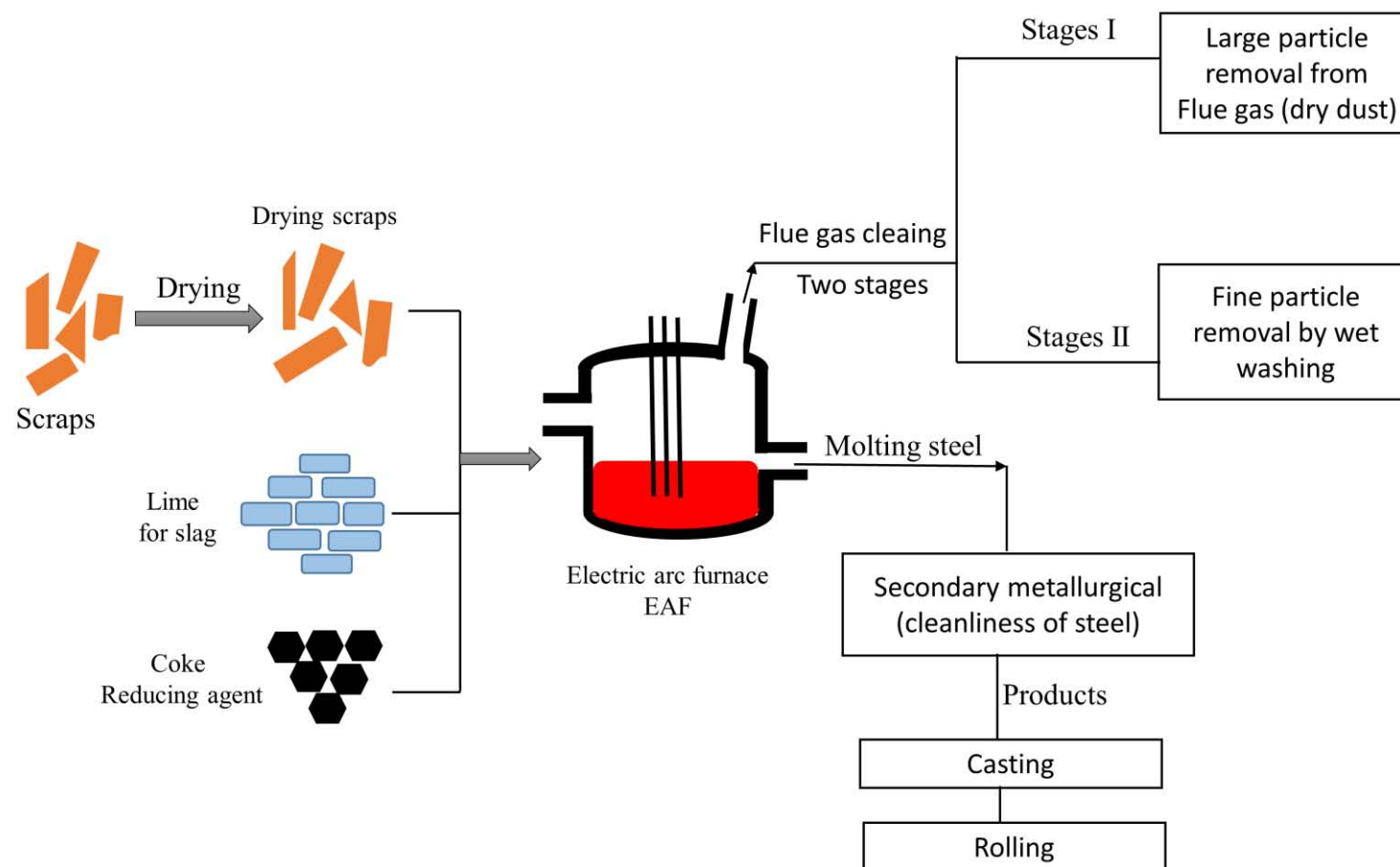


Figure 3

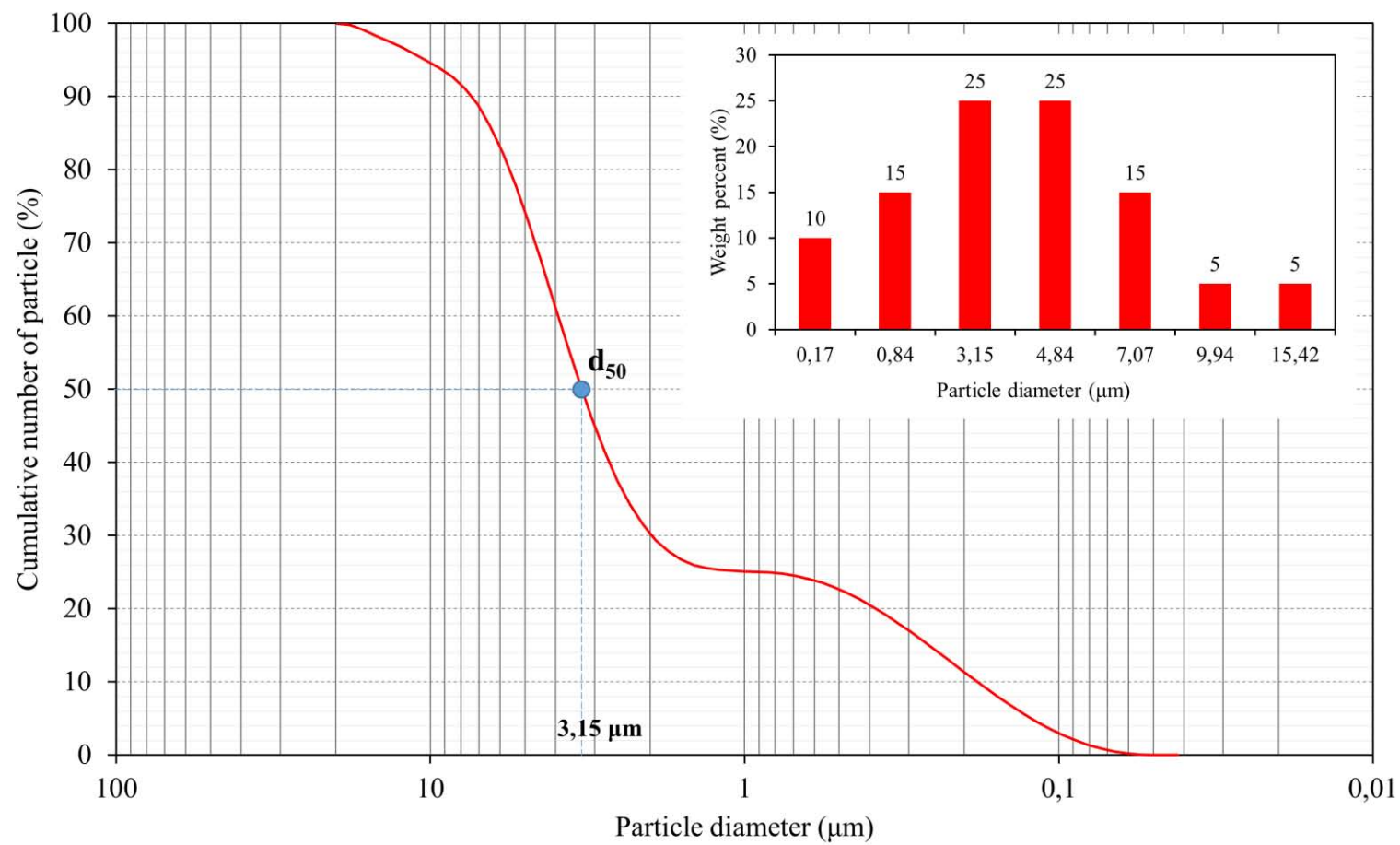


Figure 4

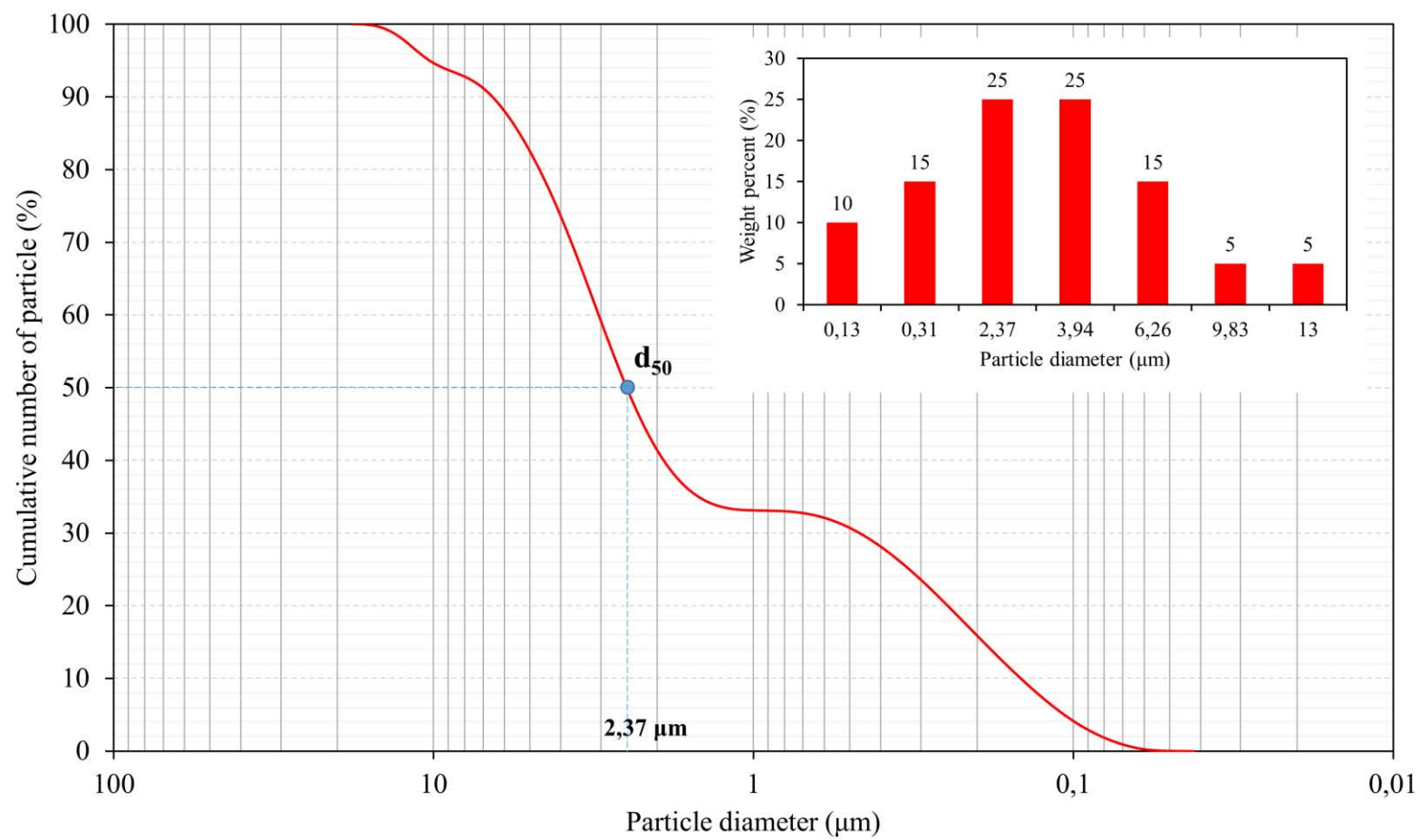


Figure 5

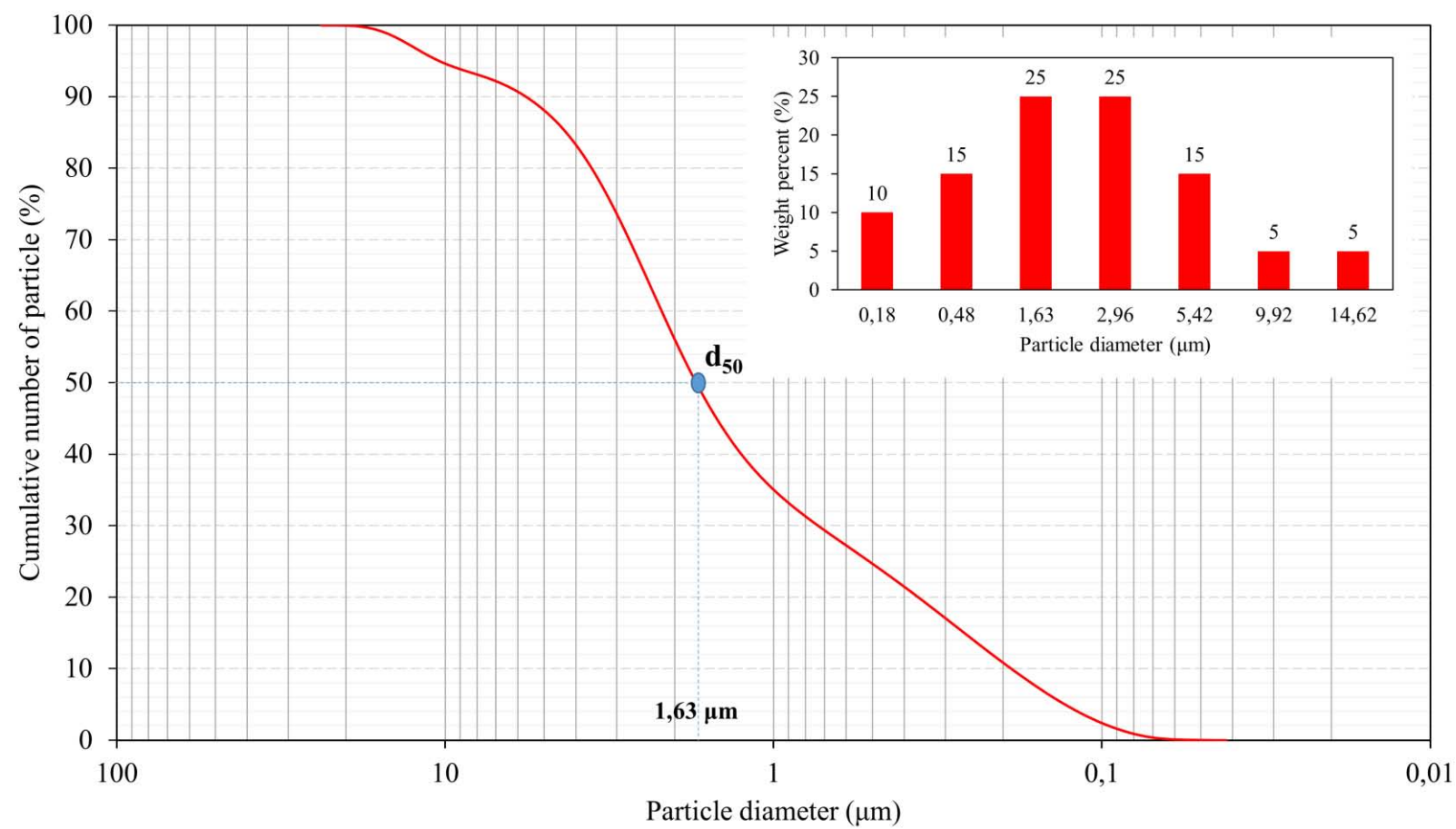


Figure 6

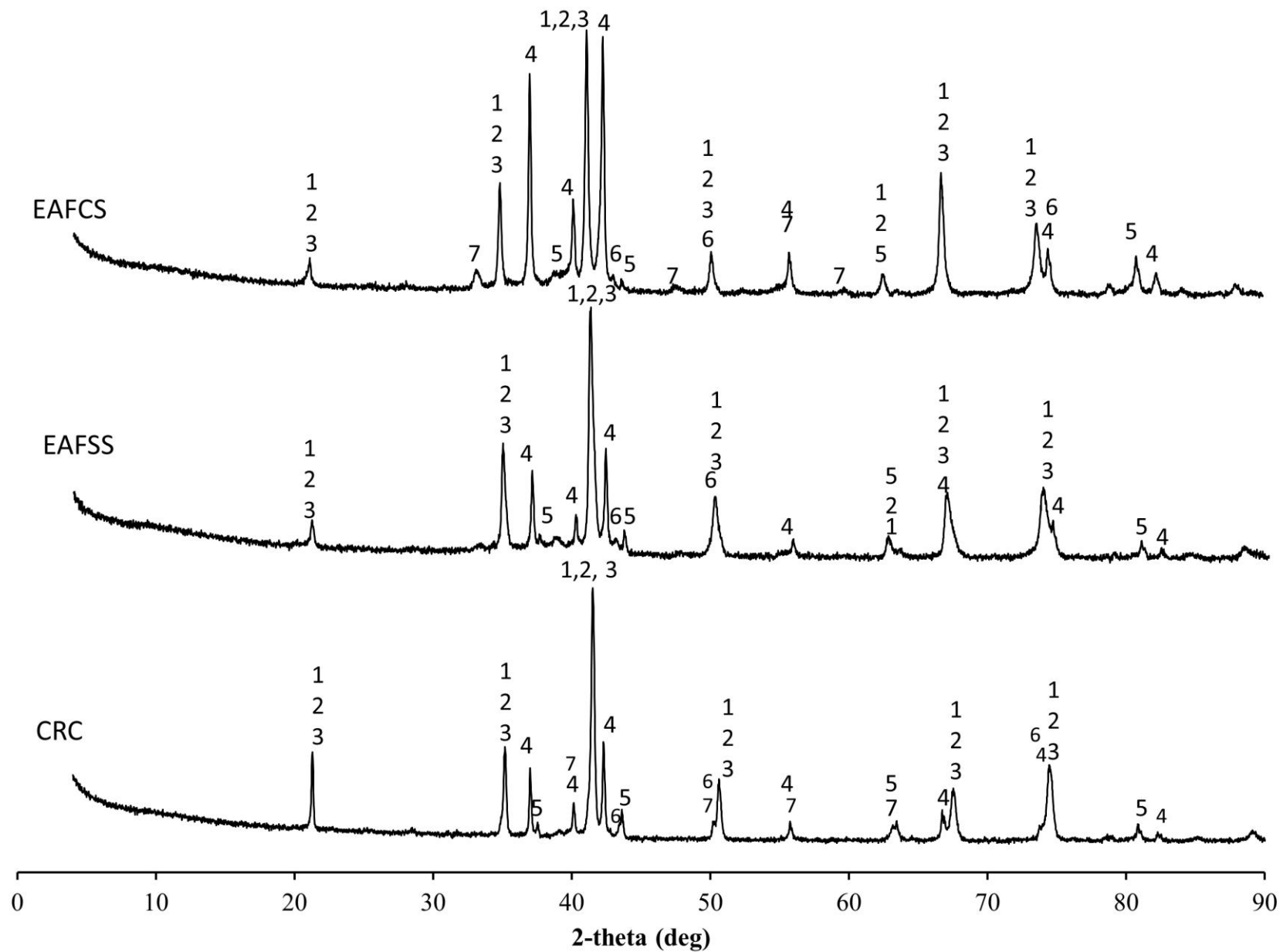


Figure 7

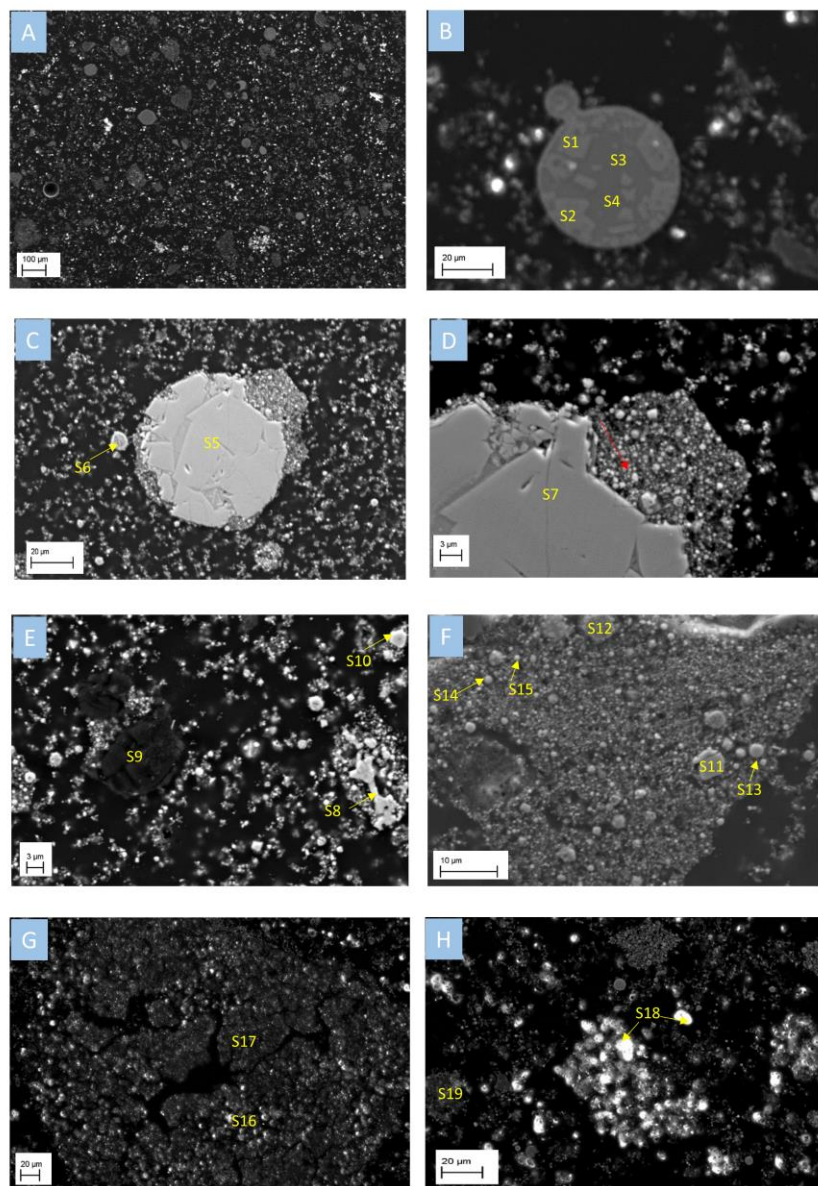


Figure 8

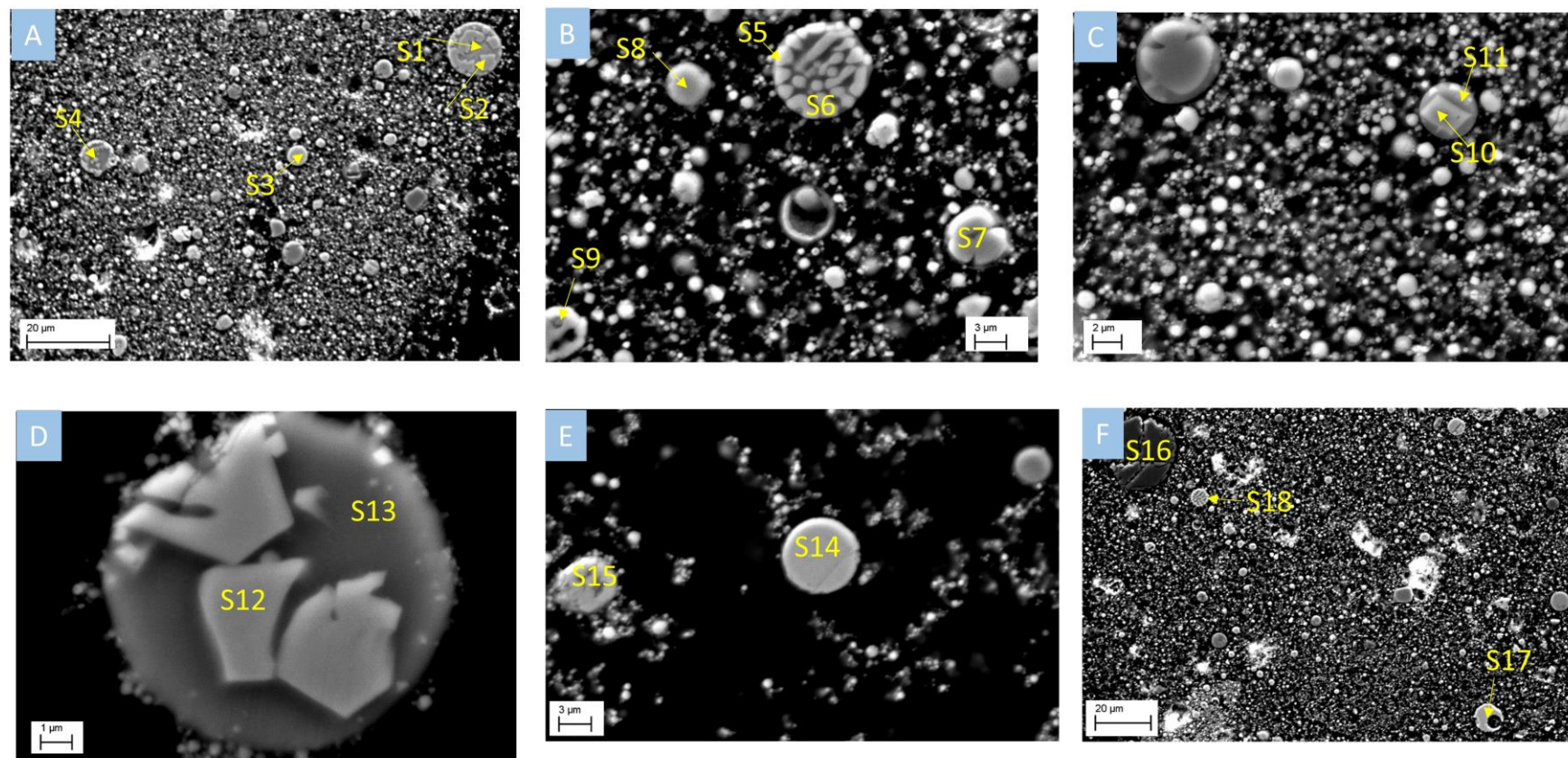


Figure 9

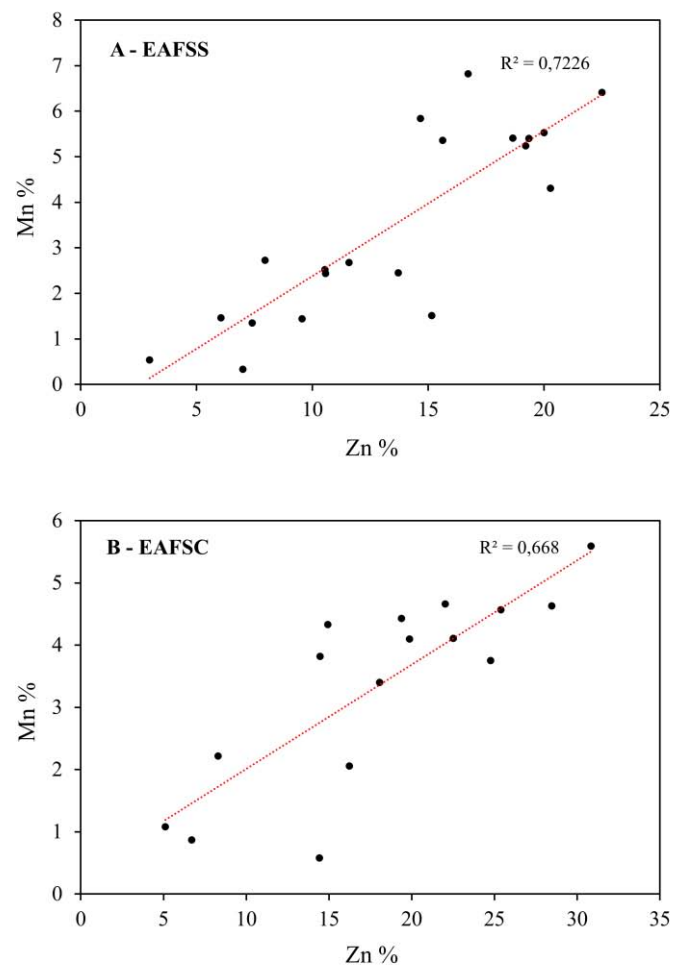


Figure 10

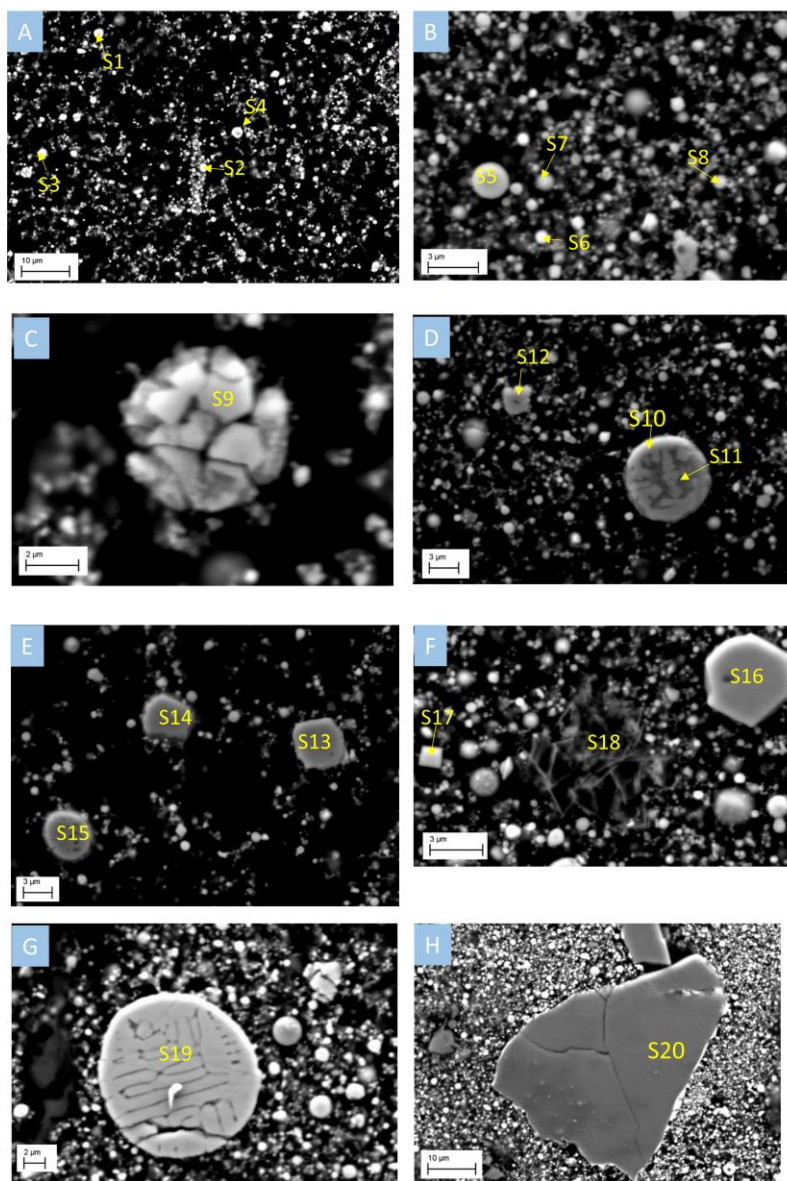


Figure 11

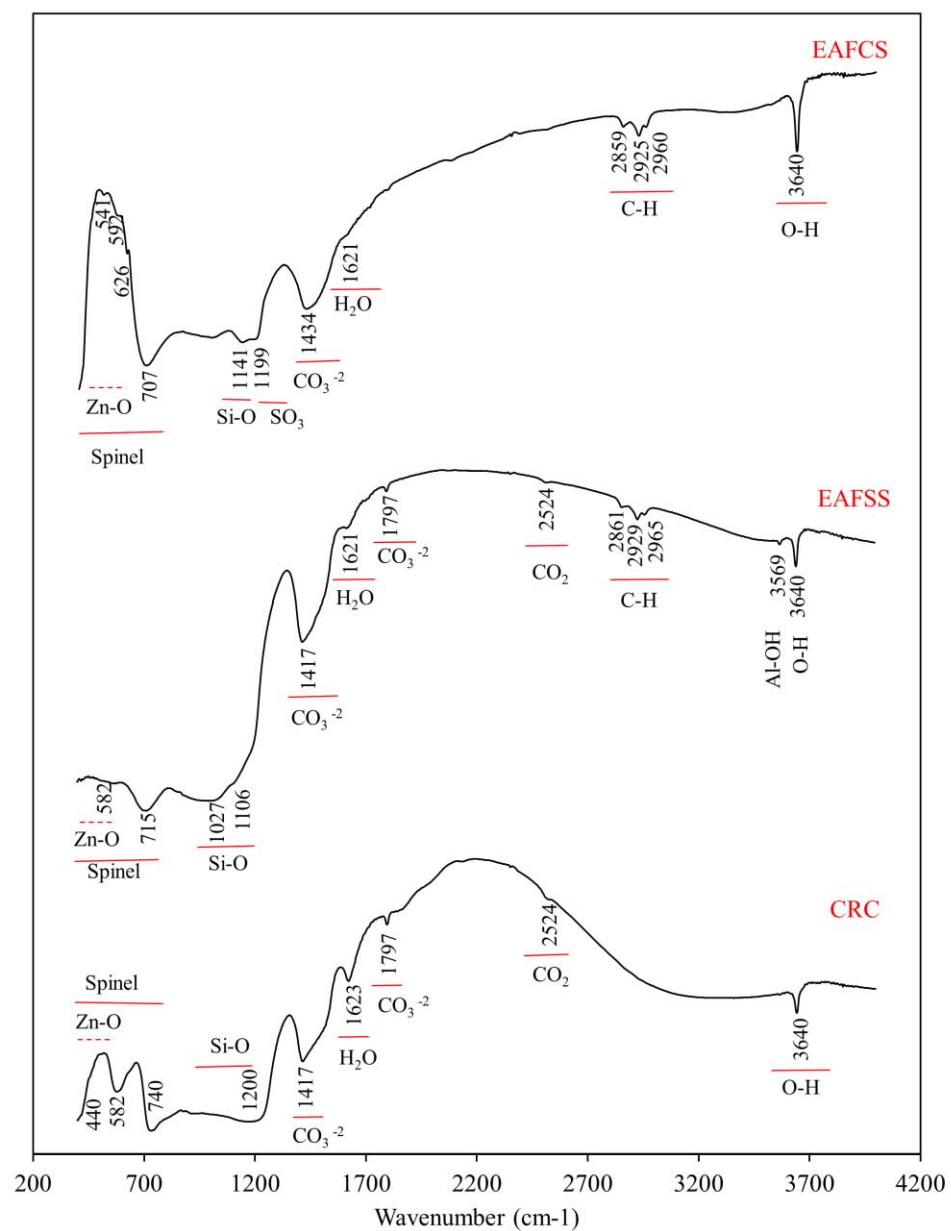


Figure 12

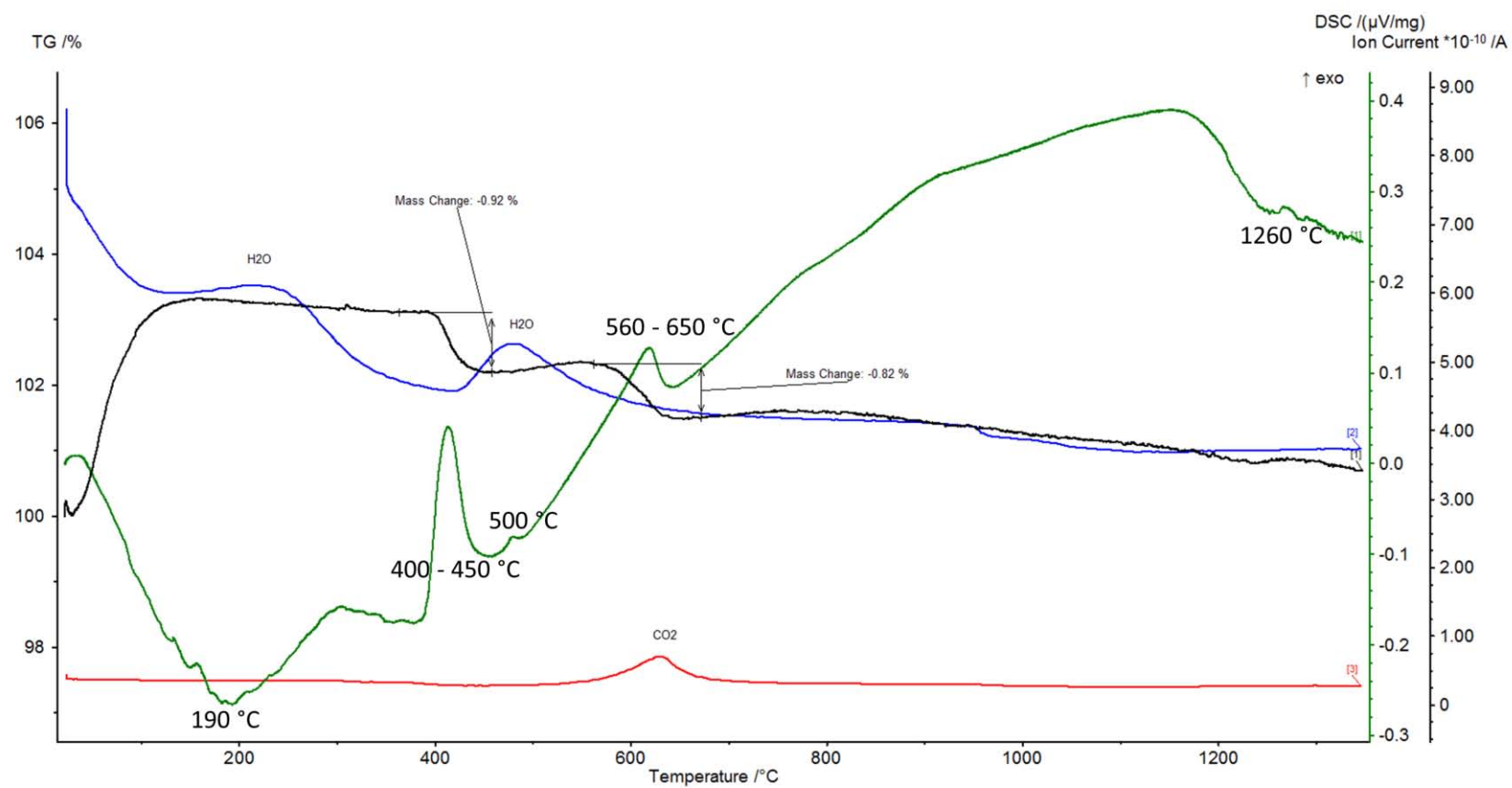


Figure 13

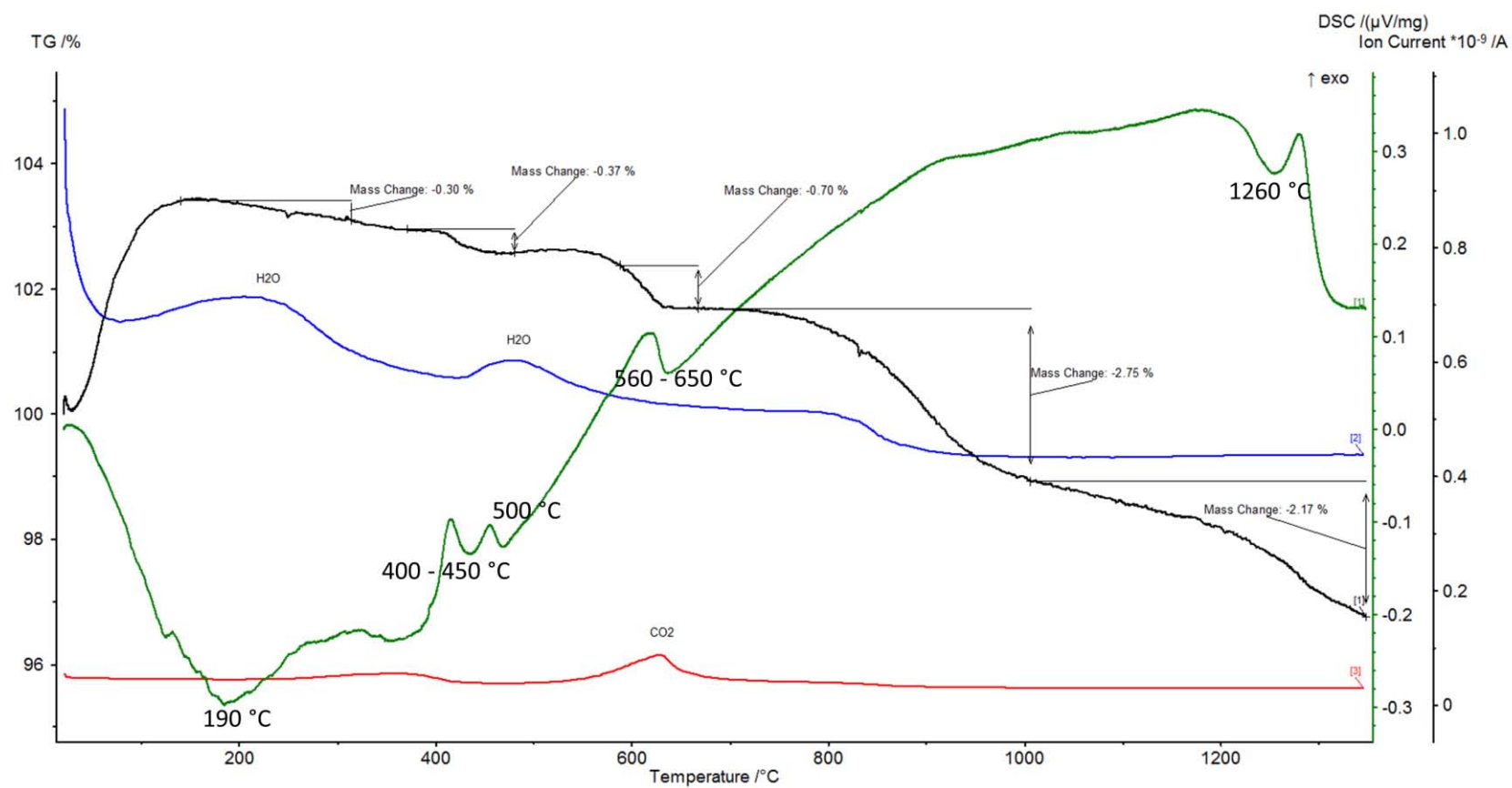
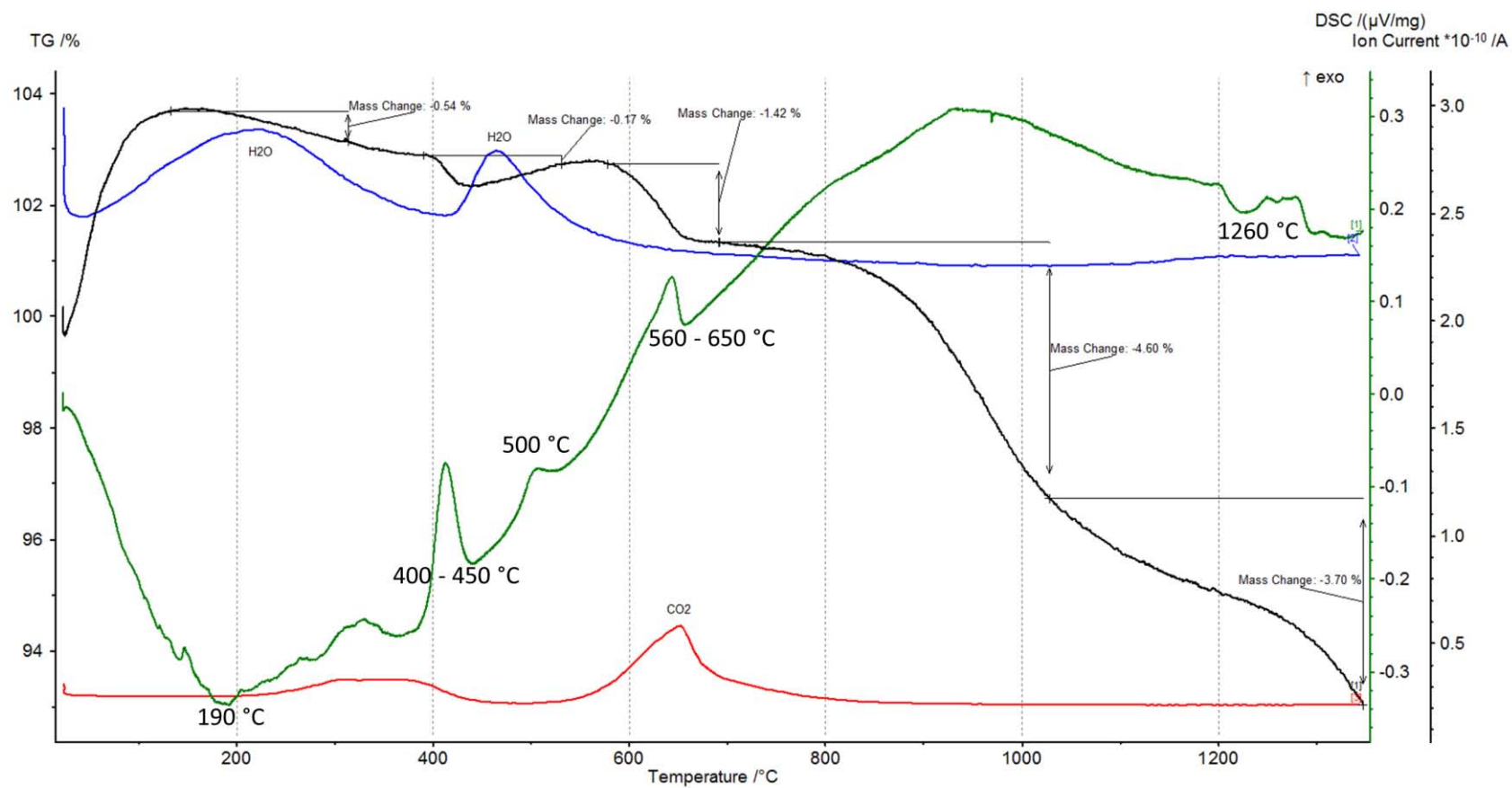
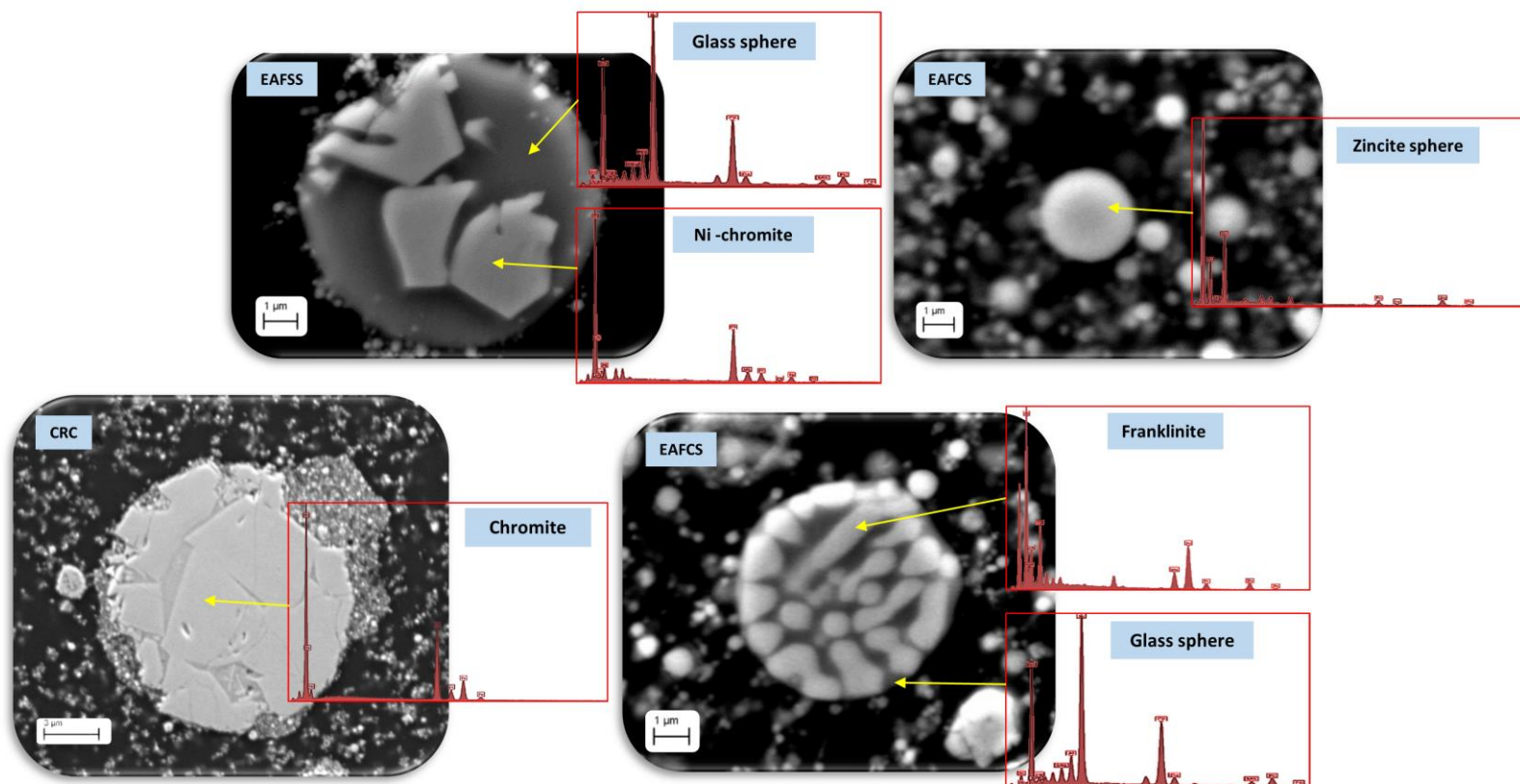


Figure 14



Graphical abstract



Effect of steelmaking dust characteristics on suitable recycling process determining: Ferrochrome converter (CRC) and electric arc furnace (EAF) dusts

Abstract

Utilization of dusts generated from steelmaking industries will avoid disposal of wastes, enhance the use of secondary raw material fines and save costs. Understanding the properties of dust is necessary before determining the suitable recycling method. The present paper describes the chemical, morphological and mineralogical characterization of steelmaking dusts produced in steel plants in Finland. In this paper three different steelmaking dusts: ferrochrome converter (CRC) and electric arc furnace stainless steel (EAFSS) dusts from Outokumpu (Tornio, Finland), and electric arc furnace carbon steel (EAFCS) dust from Ovako (Imatra, Finland) were characterized.

The characterization study showed that, the dusts from carbon steelmaking (EAFCS) are rich in zinc, while the dusts from stainless steelmaking (CRC) and (EAFSS) are relatively low in zinc, but richer in chromium. The zinc contents in CRC, EAFSS and EAFCS dusts are 10.83, 19.84 and 35.76 wt.%, respectively, while the chromium contents are 20.88, 3.19 and 0.47 wt.%, respectively. In the dust from CRC, zinc is found as zinc oxide (zincite, ZnO), while in the dusts from EAFSS & EAFCS zinc is found mostly as zinc ferrite (franklinite, ZnFe_2O_4). Scanning electron microscopy (SEM) investigations indicated that CRC dust is dominated by non-spherical form and composed mainly of aggregates of irregular particles of chromite, in addition to zincite sphere. EAFSS dust particles are characterized by encapsulation phenomenon, franklinite particles enclosed inside calcium-iron-silicate glass sphere. Manganese (Mn) concentrations shows positive correlation with Zn, which suggests the occurrence of Mn mainly with franklinite phase. EAFCS dust is dominated by spherical form, and zinc found as franklinite and zincite. In the large particles $> 3 \mu\text{m}$ of EAFCS dust, franklinite enclosed inside glass sphere, while in finer particles $< 1 \mu\text{m}$, both zincite and franklinite are existed as spheres.

The investigations indicate that steelmaking dusts from CRC, EAFSS, and EAFCS show significant difference in concentration and mode of occurrence of zinc in the dusts, which will influence on determine the suitable processing methods.

Highlights:

- Properties of steelmaking dust and its implication on determine recycling method was studied.
- EAF dust are rich in zinc, while CRC are relatively low in zinc, but richer in chromium.
- In CRC, zinc is found as zinc oxide, while in EAFSS & EAFCS zinc is found as zinc ferrite.
- Pyrometallurgical methods are more suitable for processing EAFSS and EAFCS dusts.
- Hydrometallurgical methods will be more efficient than pyrometallurgical methods for processing CRC.